


R.S. WATT
C.F. KAMINSKI
J. HULT 

Generation of supercontinuum radiation in conventional single-mode fibre and its application to broadband absorption spectroscopy

Department of Chemical Engineering, University of Cambridge, Pembroke Street, Cambridge CB2 3RA, UK

Received: 9 July 2007/Revised version: 6 September 2007
Published online: 26 October 2007 • © Springer-Verlag 2007

ABSTRACT High-pulse-energy supercontinuum radiation with a width exceeding 900 nm in the near-infrared spectral region has been generated in conventional single-mode fibre. The fibre was pumped at 1064 nm which is in the normal dispersion regime, resulting in predominantly red-shifted spectral broadening. Supercontinuum pulse energies exceeding 450 nJ were obtained. The use of conventional fibre allows for inexpensive generation of near-infrared supercontinuum radiation, featuring high pulse energies and good spatial beam quality. This supercontinuum radiation was used to acquire high-resolution (15 pm) broadband absorption spectra of H₂O, C₂H₂ and C₂H₄ in the near-infrared spectral region (1340–1700 nm), using an optical spectrum analyser for detection. H₂O spectra were also recorded at high repetition rates, by dispersing the supercontinuum pulses and detecting the transmitted signal in the time domain. A spectral resolution of 38 pm was obtained employing the dispersed supercontinuum pulses, which is comparable to the H₂O line widths at ambient conditions.

PACS 07.07.Df; 42.62.Fi; 42.79.Nv; 42.81.-i

1 Introduction

Broadband light sources are attractive for many practical spectroscopic applications, for example as sensors for gas or liquid properties, for optical component and system testing or for biological imaging. Broadband wavelength coverage ensures that spectral signatures of multiple species or compounds can be detected or that optical properties of components can be characterized over broad bandwidths. Supercontinuum (SC) light sources are of particular interest in this context, as they can provide broadband pulses covering extremely wide wavelength ranges [1]. Supercontinuum light sources have successfully been employed for gas sensing [2–4], optical component characterization [5–7], optical coherence tomography [8] and confocal microscopy [9, 10]. Rapid wavelength sweeping can be achieved by stretching the supercontinuum pulses using dispersive fibres, which allows such broadband measurements to be performed very quickly [2, 3, 11–13].

Intense laser pulses have been used to generate broadband supercontinuum radiation in solids, fluids and gases, through a variety of non-linear optical processes [1]. Of particular interest to practical applications is the high efficiency of supercontinuum generation in optical fibres [14]. Normally photonic crystal fibres (PCFs) [15] or highly non-linear fibres (HNLFs) [16] are employed for this purpose. The small core diameter of such fibres enhances the non-linear processes, and allows broadband supercontinuum generation at sub-nJ pulse energies when pumped by femto- or picosecond laser pulses. However, the reduced threshold of optical damage in those narrow-core fibres limits the maximum pulse energy that it is possible to obtain in the supercontinuum (typically to less than 100 nJ for pumping with pulses less than 10-ps long), which limits their usefulness for some practical applications where higher pulse energies are required. Standard single-mode fibres, on the other hand, exhibit a higher optical damage threshold and have successfully been employed for generation of high-pulse-energy (μ J) supercontinuum pulses in the visible [17–19] and near-infrared (IR) spectral regions [18–22]. Supercontinuum radiation generated in standard single-mode fibres is furthermore characterized by a better spatial beam profile, compared to supercontinua generated in PCFs, which normally feature a non-circular symmetry. Other advantages of employing conventional fibre include low cost and ease of splicing. Supercontinuum generation in standard single-mode fibres has recently also been demonstrated in the UV [23] and mid-IR [24, 25] spectral regions.

This paper investigates the generation of high-pulse-energy near-IR supercontinuum radiation in standard telecom fibre, and reports the application of such high-pulse-energy supercontinuum radiation to broadband absorption spectroscopy in gases. In this study standard telecommunication-grade fibre is pumped in the normal dispersion regime of the fibre, at 1064 nm [19], which results in a predominantly red-shifted supercontinuum exhibiting a good flatness from 1300 nm to 1700 nm. The effects of changing the energy of the pump pulse and the fibre length on the spectral shape of the supercontinuum are investigated. The red-shifted supercontinuum is ideal for gas sensing as many molecules of practical interest feature vibrational overtone transitions in the near-IR region [26]. Its usefulness for spectroscopic applications is demonstrated by obtaining broadband and high-resolution (15 pm) absorption spectra of the H₂O band stretching from

✉ Fax: +44-1223-334796, E-mail: jfh36@cheng.cam.ac.uk

1340 nm to 1500 nm, the C_2H_2 band stretching from 1510 nm to 1545 nm and the C_2H_4 band stretching from 1610 nm to 1700 nm. The spectral resolution obtained is better than that previously reported for supercontinuum-based spectrometers [2–4, 12] and allows the ro-vibrational structure of those molecules to be resolved. Finally, broadband H_2O spectra are also recorded at much higher repetition rates, by dispersing the supercontinuum pulses and detecting the resulting spectral sweeps in the time domain [2, 3]. The type of broadband absorption spectrometer presented here shows large promise for multi-species concentration and temperature measurements, with future potential of reactive flow sensing.

2 Instrumentation

The experimental configuration employed for characterizing the spectral characteristics of the supercontinuum radiation generated in the single-mode fibre, and for recording broadband absorption spectra of various gases, is schematically illustrated in Fig. 1a. The supercontinuum radiation is generated by launching 5-ps-long pulses, centred around 1064 nm, into a single-mode fibre (SMF, Corning, SMF28). At 1064 nm the SMF28 fibre features a dispersion of around -30 ps/(nm km) and a mode field diameter of around 7.5 μ m. Its zero-dispersion wavelength (ZDW) is located at 1313 nm, and the cut-off wavelength is around 1260 nm. The pump laser is an ytterbium-doped fibre laser (Fianium, FemtoPower-1060) featuring an acousto-optical pulse picker which allows the repetition rate to be varied between 0.33 MHz and 20 MHz. The maximum pulse energy that it is possible to obtain increases from 45 nJ at 20 MHz to over 1.4 μ J at 0.33 MHz repetition rate. An aspherical lens was used for coupling light into the single-mode fibre, with a typical coupling efficiency of 33%.

For initial characterization of the supercontinuum radiation, the spectral output from the fibre was directly recorded

by an optical spectrum analyser (OSA, Ando, AQ6317Q). To allow the widest range of pump pulse energies to be tested the lowest repetition rate (0.33 MHz) was employed. The output power of both the pump laser and the supercontinuum radiation was monitored using a broadband power meter (Melles Griot, 13 PEM 001).

The same set-up was employed for recording broadband absorption spectra, by collimating the SC into a 4-mm-diameter beam, launching it through the gas sample (H_2O , C_2H_2 or C_2H_4) to be analysed and then re-launching it back into a single-mode fibre for subsequent detection using the OSA. The spectral resolution of the OSA is specified to be around 15 pm, between 1520 and 1620 nm, which is sufficiently high to resolve individual ro-vibrational lines of many gaseous species in the near-IR spectral region.

Absorption measurements of H_2O vapour were also carried out in the time domain by dispersing and resolving the individual SC pulses, using the set-up illustrated in Fig. 1b. This was achieved by employing two dispersion-compensating modules (DCMs), each featuring a dispersion which varies from -0.9 ns/nm at 1300 nm to -1.5 ns/nm at 1500 nm (Fujikura, G652-C+L-band SC-DCFM). The wavelength-dependent dispersion of the modules has been accurately characterized using a time-of-flight method developed by the authors [7]. The resulting output from the two DCMs is a rapid wavelength scan, which sweeps from 1300 nm to 1500 nm in approximately 180 ns. The SC beam is then passed through the gas sample to be analysed and the transmitted intensity is detected using a 10-GHz-bandwidth pre-amplified photodiode (Terahertz Technologies, TIA-3000) connected to a 8-GHz-bandwidth real-time oscilloscope (Tektronix, TDS6804B). The spectral resolution is determined by the amount of dispersion employed. Here two DCMs were used to achieve a resolution of around 38 pm, which approximately matches the width (33 pm) of the H_2O lines studied.

3 Results and discussion

3.1 Supercontinuum generation

By employing sufficiently intense laser pulses it is possible to generate broadband supercontinuum radiation in conventional single-mode fibres, even though their non-linear coefficient is lower than that of PCFs and HNLFs. The SMF employed here has a zero-dispersion wavelength of 1313 nm, which is about 250 nm above the pump wavelength, which means that pumping is performed well inside the normal dispersion regime, where solitons cannot be formed. The spectral profile of the SC is studied as a function of the energy of pulses injected into the fibre and as a function of the length of fibre employed. In this work the prime objective was to maximize the intensity in the region stretching from 1300 nm to 1700 nm, as this is a region of interest for near-IR absorption spectroscopy.

In Fig. 2a the spectral profile of the supercontinuum as a function of pulse energy is shown for the case of a 10-m-long fibre. In Fig. 2b the corresponding intensity map illustrating the evolution of the supercontinuum as a function of pulse energy is shown. For the lowest pulse energy, 30 nJ, the spectral profile essentially mimics that of the pump laser. The pump laser has a spectral full width at half maximum (FWHM) of

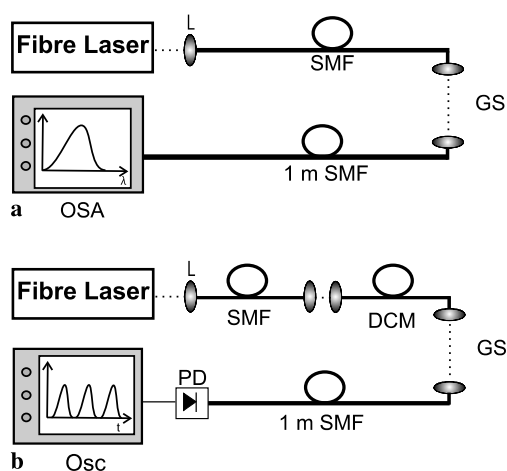


FIGURE 1 (a) Optical set-up used for characterizing the spectral profile of the generated supercontinuum and for recording broadband absorption spectra of various species. (b) Experimental set-up used for rapid acquisition of broadband H_2O spectra. The dispersed supercontinuum sweeps were recorded in the time domain by a photodiode and a real-time oscilloscope. (L = lens, SMF = single-mode fibre, OSA = optical spectrum analyser, DCM = dispersion-compensating module, GS = gas sample, PD = photodiode, Osc = oscilloscope)

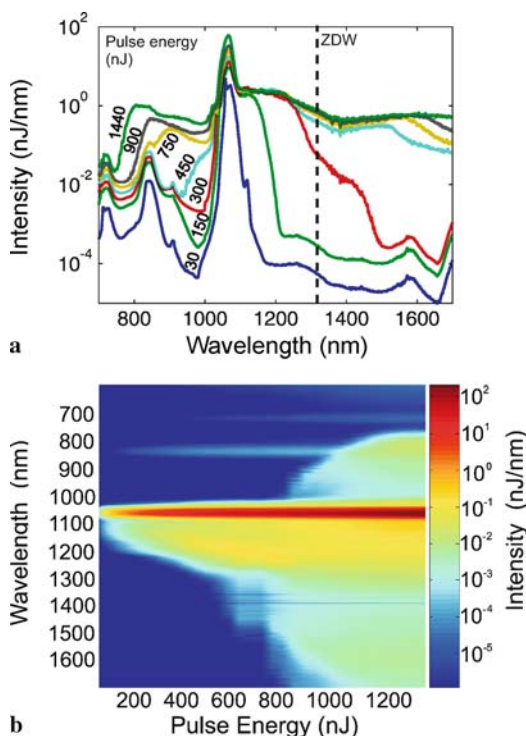


FIGURE 2 (a) Spectral profile of supercontinuum radiation generated in a 10-m-long conventional single-mode fibre shown as a function of pulse energy (ZDW = zero-dispersion wavelength). (b) Corresponding spectral intensity map (logarithmic intensity scale)

around 18 nm with a weak wing extending to higher wavelengths, which is caused by stimulated Raman scattering inside the fibre laser. The supercontinuum generation starts to take place at a pump energy of around 150 nJ. As the pump wavelength lies in the normal dispersion regime in this case it is thought that self-phase modulation in combination with stimulated Raman scattering initiates the formation of the SC. As the energy of the injected pulses is increased cascaded Raman shifting extends the SC towards the anomalous dispersion regime, i.e. above the ZDW at 1313 nm. When the pulse energy is increased from 300 nJ to 450 nJ a rapid broadening towards higher wavelengths is observed. Further increases in pulse energy increase the intensity of the supercontinuum radiation above 1500 nm, and also lead to the emergence of radiation on the shorter-wavelength side of the pump laser. The principal features of the spectral envelope of the supercontinuum are similar to those reported by Chernikov et al., and the physical processes responsible for the spectral broadening are believed to be similar to those identified in that study [19, 27]. The fine scale structure visible around 1400 nm is due to absorption by ambient H₂O vapour present inside the spectrum analyser. The two weak peaks around 725 nm and 850 nm have been confirmed to be measurement artifacts caused by the OSA.

The effect of varying the fibre length is shown in Fig. 3, where the maximum pulse energy (1440 nJ) was employed for all lengths. For fibre lengths of 1 m and 2 m the spectral profiles observed closely resemble that of the pump laser, which indicates that a fibre length longer than 2 m is required for effective SC generation to take place in the present case. When the fibre length is increased to 5 m or longer increased spectral

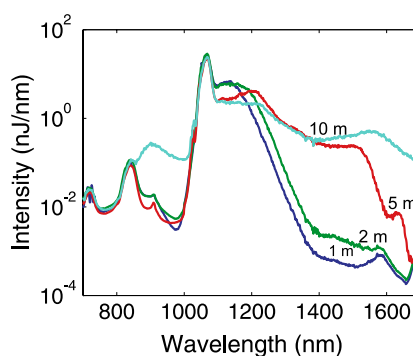


FIGURE 3 Spectral profile of the supercontinuum radiation generated in different lengths of conventional fibre

broadening is observed. About 33% and 44%, respectively, of the energy is converted to higher wavelengths for the 5-m- and 10-m-long fibres. The use of fibres longer than 10 m did not improve the spectral width of the SC to any greater extent. For this reason a 10-m-long fibre was employed for the absorption measurements described in this paper.

At maximum pulse energy the supercontinuum generated in the 10-m-long fibre spans over 900 nm in width (measured between the -20 dB points), with 23% of the energy being transferred into the 1300–1700 nm window of interest. The relatively high intensity and flat spectral profile in this region make this ideal for near-IR absorption spectroscopy of gaseous species.

3.2 Spectrally resolved absorption spectroscopy

To demonstrate the usefulness of the high-pulse-energy supercontinuum source for broadband absorption spectroscopy, spectra of vibrational overtone and combination bands in H₂O, C₂H₂ and C₂H₄ were recorded at ambient conditions. From the transmitted (I) and incident (I_0) intensities the absorbance A can be calculated:

$$A = \log(I_0/I). \quad (1)$$

The ratio between transmitted and incident intensities is given by the Beer–Lambert law, from which the number density N can be determined:

$$I/I_0 = \exp(-\sigma(\lambda)NL), \quad (2)$$

where $\sigma(\lambda)$ is the absorption cross section for the transition studied, and L is the path length. In Fig. 4a the transmitted intensity (I) of the SC after passing through approximately 2.8 m of air is shown. The transmission trace, which stretches from 1340 nm to 1500 nm, was acquired using the OSA and covers the entire ro-vibrational structure of the H₂O band, containing over 400 individual absorption features. In Fig. 4b the corresponding absorption spectrum is shown, which was obtained by fitting a base line (I_0) to the transmission trace and applying (1). The ambient conditions were a temperature of 297 K, a pressure of 1001 mbar and a relative humidity (RH) of 39%, which yield a H₂O mole fraction of $X_{\text{H}_2\text{O}} = 0.0116$. A calculated spectrum corresponding to the experimental conditions and based on line strength and line shape data from the HiTran 2004 database [28] is shown in

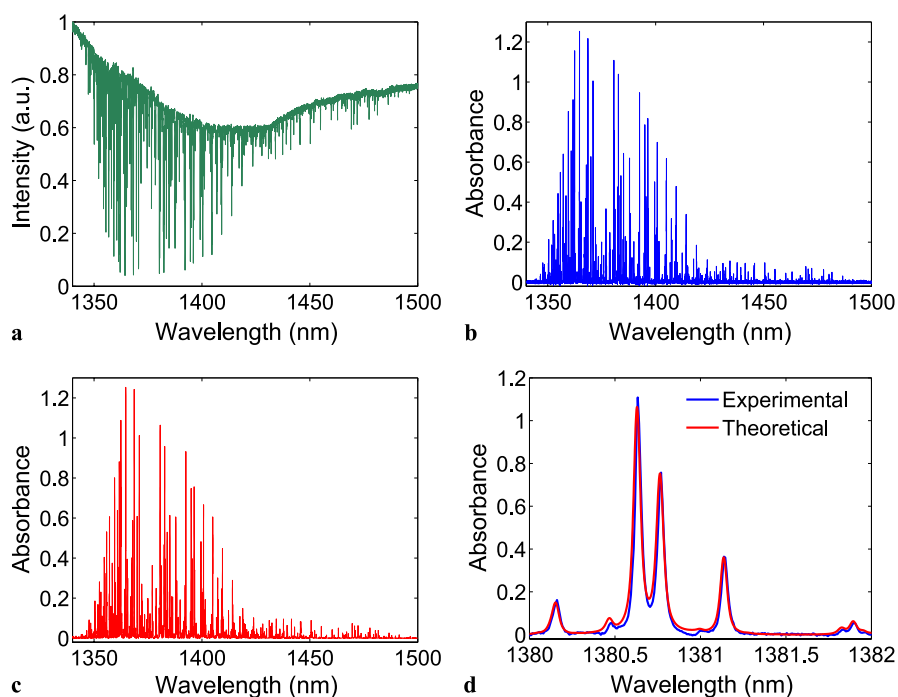


FIGURE 4 (a) Intensity of the SC radiation transmitted through air with a relative humidity of 39%, recorded using an OSA. The absorption lines observed are vibrational overtone transitions of H_2O . (b) Corresponding H_2O absorbance spectrum. (c) Theoretical spectrum calculated using line parameters from the HiTran database at the experimental conditions ($L = 2.8$ m, $T = 297$ K, $P = 1001$ mbar, $\text{RH} = 39\%$, $X_{\text{H}_2\text{O}} = 0.0116$). (d) Magnified view of the 1380–1382 nm region, showing both experimental and HiTran H_2O peaks

Fig. 4c. To allow a direct comparison between the experimental and the HiTran spectra, the latter has been convolved with a Gaussian filter with a width of 15 pm, corresponding to the spectral resolution of the OSA. Overall, the two spectra are seen to agree well, which is further evident from the magnified view shown in Fig. 4d. The observed signal-to-noise ratio, based on the strongest peak, was around 135. The detection limit using the OSA for acquisition, for the strongest H_2O peak in Fig. 4b, was estimated to be around 135 ppm for a 1-m absorption path length at room temperature and atmospheric pressure.

Broadband absorption measurements were also performed in a gas mixture of C_2H_2 and CO ($\sim 0.75\%$ C_2H_2) contained in a 14-cm-long cell. The experimentally recorded spectrum is shown in Fig. 5a; C_2H_2 absorption features stretching from 1510 to 1545 nm are observed, corresponding to the vibrational combination band $\nu_1 + \nu_3$. Once again the recorded spectrum was compared with a spectrum calculated based on line parameters from the HiTran database, which is shown in Fig. 5b. A good agreement between experimental and theoretical results is observed, as is evident from the magnified view shown in Fig. 5c.

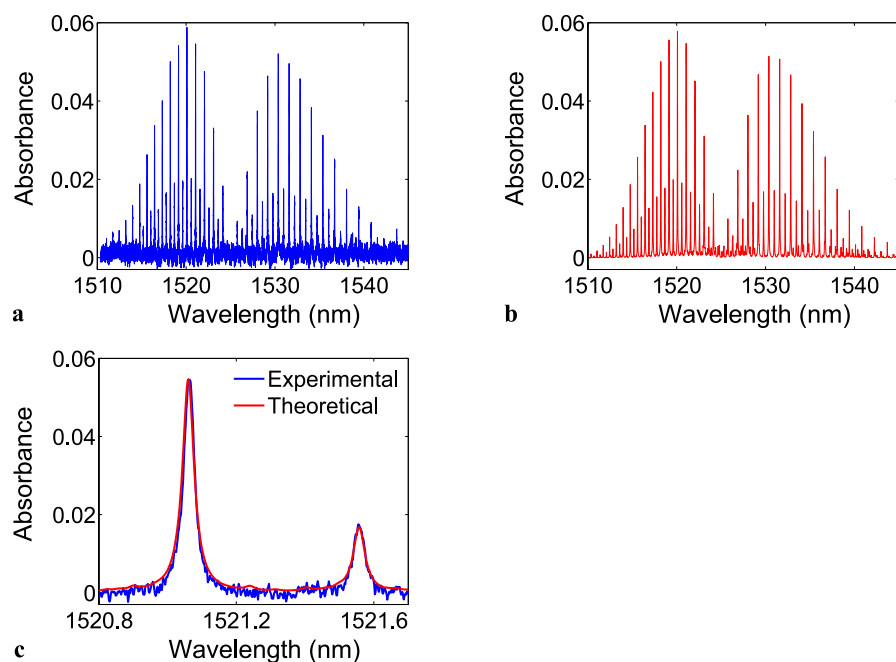


FIGURE 5 (a) Experimental C_2H_2 absorption spectrum covering the entire vibrational combination band ($\nu_1 + \nu_3$) of C_2H_2 . (b) Theoretical spectrum calculated using line parameters from the HiTran database at the experimental conditions ($L = 14$ cm, $T = 297$ K, $P = 1001$ mbar, $X_{\text{C}_2\text{H}_2} \approx 0.007$). (c) Magnified view of the 1520.8–1521.8 nm region

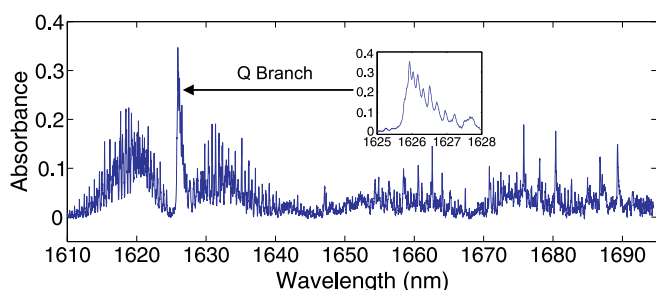


FIGURE 6 Experimental absorption spectrum of C_2H_4 stretching from 1610 nm to 1700 nm. *Inset*: Q-branch of the $\nu_5 + \nu_9$ combination band shown in magnification

The third test object consisted of a 10.5-cm-long path of pure C_2H_4 . A 90-nm-wide spectrum of C_2H_4 is shown in Fig. 6. The P-, Q- and R-band structure around 1625 nm corresponds to the $\nu_5 + \nu_9$ combination band, whereas the lines above 1640 nm correspond to a number of overlapping combination bands [29]. As the HiTran database does not contain spectroscopic data for those near-IR transitions of C_2H_4 a direct comparison to a theoretical spectrum is not possible. However, the observed structure is in good agreement with the broadband spectrum published by Boschetti et al. [30]. Furthermore, the distinct Q-branch of the $\nu_5 + \nu_9$ transition, shown in the inset of Fig. 6, agrees well with that measured by Sanders et al. [31].

3.3 Temporally resolved absorption spectroscopy

Employing a scanning grating based spectrometer such as an OSA for detection is time consuming and therefore temporally resolved time-of-flight absorption measurements, which can be performed at much higher repetition rates, are

desirable [2, 3]. Temporally resolved data is acquired by first dispersing the individual SC pulses and then capturing the resulting wavelength sweeps using a high-bandwidth photodiode and real-time oscilloscope. This technique is demonstrated here by launching the dispersed SC through a 1.9-m-long path of ambient air and recording the H_2O absorption spectrum. The transmitted intensity as a function of arrival time at the detector is shown in Fig. 7a. The transmission trace shown corresponds to an average of 1000 individual wavelength sweeps. By detailed knowledge of the DCM dispersion curve [7] the instantaneous wavelength scale could be determined, which is shown on the upper axis of Fig. 7a.

An absorbance spectrum is calculated from the recorded transmission trace (I) and the fitted baseline (I_0) and is shown in Fig. 7b. The spectral resolution of the dispersed supercontinuum measurement is determined by the dispersion employed and by the electronic bandwidth of the detection and acquisition system. By using two DCM modules for dispersing the SC a spectral resolution of around 38 pm was achieved, which is close to the H_2O line width of about 33 pm at ambient conditions. This means that the observed spectral lines are slightly under-resolved. In Fig. 7c a calculated spectrum corresponding to the experimental conditions is shown. This spectrum has been convolved with a Gaussian filter, the width of which corresponds to the experimentally determined spectral resolution, to allow a direct comparison.

The H_2O concentration was determined from the experimental absorption spectrum shown in Fig. 7 by fitting the HiTran spectrum to the experimental spectrum. As part of this procedure the intensity, centre position and width of each individual HiTran peak is fitted. The entire fitting procedure was performed directly in the transmitted intensity trace (Fig. 7a), in order to preserve the line strength of each peak when convolved with the Gaussian filter which controls the line width.

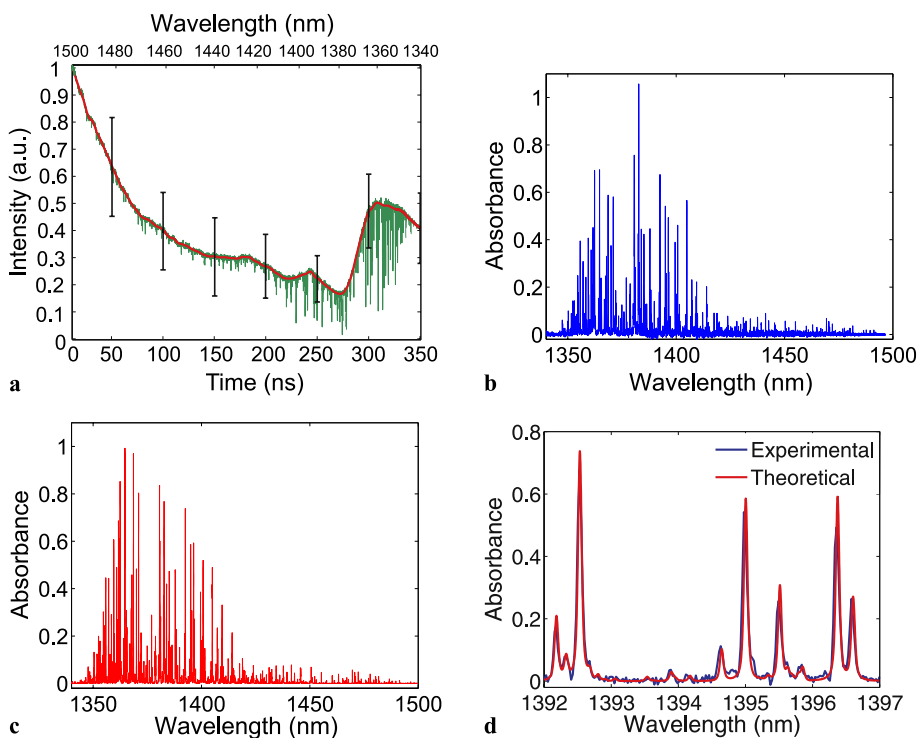


FIGURE 7 (a) Intensity of the dispersed SC pulses, transmitted through air with a relative humidity of 47%, and captured using a high-bandwidth photodiode and a high-bandwidth oscilloscope. The *green line* corresponds to an average of 1000 wavelength scans; the standard deviation of the transmitted intensity is indicated by the *error bars*. The baseline fitted to the transmission trace is shown in *red*. (b) Corresponding H_2O absorbance spectrum. (c) Theoretical spectrum calculated using line parameters from the HiTran database at the experimental conditions ($L = 1.9$ m, $T = 296$ K, $P = 1001$ mbar, $RH = 47\%$, $X_{H_2O} = 0.0133$). (d) Magnified view of the 1392–1397 nm region, showing both experimental and HiTran H_2O peaks

The thus obtained average intensity scaling factor (1.024 in the present case) allowed the H₂O mole fraction to be determined to be $X_{\text{H}_2\text{O}} = 0.0136$. The mole fraction of H₂O present in air was calculated to be $X_{\text{H}_2\text{O}} = 0.0133$, based on measured temperature (296 K) and relative humidity (47%). The observed discrepancy of only 2.4% is within the accuracy of the hygrometer employed, and demonstrates the feasibility of rapid concentration measurements, based on this type of broadband absorption sensor.

The experimental spectra presented here were acquired by averaging 1000 wavelength sweeps, resulting in a total acquisition time of about 3 ms as the repetition rate employed was 0.33 MHz. This acquisition rate is almost a factor of 5000 times greater than that achieved using the OSA. The use of shorter averages would of course offer the possibility of even higher repetition rates, albeit at the expense of reduced signal-to-noise ratios. The pulse-to-pulse variations in the supercontinuum profile are indicated by the error bars in Fig. 7a, which correspond to the observed standard deviation of the intensity profile. The fluctuations are quite large, with a relative standard deviation of about 40% at the centre of the spectrum. The quality of single-sweep spectra is further degraded by acquisition noise, which is the dominant source of noise in the present case where the use of two DCMs leads to relatively low powers reaching the detection system. Reduced optical losses, for example achieved through the use of fibre splicing rather than free space coupling as currently used, in the experimental set-up could thus lead to improved signal-to-noise ratios in the future. In this context it is interesting to note that the use of a single DCM results in sufficient signal to allow this type of concentration measurement to be performed at rates exceeding 100 kHz, as recently demonstrated for the case of CH₄ [32]. Other sources of noise influencing this type of rapidly wavelength swept measurement include photon noise and beating noise [33]. In the averaged spectrum shown in Fig. 7 the signal-to-noise ratio was observed to be about 100 for the strongest peak. The detection limit for the temporally resolved approach, for the strongest H₂O peak in Fig. 7b, was estimated to be around 500 ppm for a 1-m absorption path length at room temperature and atmospheric pressure.

4 Conclusion

Near-IR supercontinuum radiation suitable for broadband spectroscopic applications has been generated in conventional single-mode fibre by pumping at 1064 nm, in the normal dispersion regime of the fibre. The resulting supercontinuum radiation, which is predominantly red shifted from the pump wavelength, extends from 800 nm to beyond 1700 nm.

The high pulse energy (> 450 nJ) and the relatively flat spectral profile between 1300 nm and 1700 nm, where many smaller molecules feature vibrational overtone transitions, make this light source suitable for gas-phase spectroscopy. High-resolution (15 pm) spectra of H₂O, C₂H₂ and C₂H₄ were obtained in the 1340 nm to 1700 nm region, using an optical spectrum analyser for detection. The spectra were observed to be in good agreement with theoretical spectra, and clearly demonstrate the capability of broadband absorption spectroscopy. Finally, the SC pulses were also dispersed in time

to carry out time-resolved absorption measurements at much higher repetition rates. This technique was demonstrated by recording 160-nm-wide H₂O spectra with a spectral resolution of 38 pm at a repetition rate of 330 Hz.

We believe that the type of high-pulse-energy supercontinuum pulses obtained is highly suitable for rapid broadband absorption sensing in a range of applications. The experimental set-up employed is simple and can be entirely fibre coupled, making it relatively compact and easily transportable. Future applications in various types of flames and combustors are envisaged, where concentrations of multiple species could be probed in real time. The capability of acquiring spectra covering a large number of H₂O absorption lines also opens up the possibility of measuring temperature distributions in flames, as described by Liu et al. [34].

ACKNOWLEDGEMENTS This work was supported by Research Grants from the UK Engineering and Physical Sciences Research Council (EPSRC: EP/C012488/1) and from the Royal Society. J.H. was supported by an Advanced Research Fellowship (EP/C012399/1) from the EPSRC, and CFK would like to thank the Leverhulme Trust for personal sponsorship.

REFERENCES

- 1 A.R. Alfano (ed.), *The Supercontinuum Laser Source*, 2nd edn. (Springer, New York, 2006)
- 2 P.V. Kelkar, F. Coppinger, A.S. Bhushan, B. Jalali, *Electron. Lett.* **35**, 1661 (1999)
- 3 S.T. Sanders, *Appl. Phys. B* **75**, 799 (2002)
- 4 C. Lan, A.W. Caswell, L.A. Kranendonk, S.T. Sanders, *Tech. Paper 2007-01-0188*, SAE International (2007)
- 5 M. Lehtonen, G. Genty, H. Ludvigsen, *Appl. Phys. B* **83**, 231 (2005)
- 6 F. Koch, S.V. Chernikov, J.R. Taylor, *Opt. Commun.* **175**, 209 (2000)
- 7 J. Hult, R.S. Watt, C.F. Kaminski, *J. Lightwave Technol.* **3**, 820 (2007)
- 8 I. Hartl, X.D. Li, C. Chudoba, R.K. Ghanta, T.H. Ko, J.G. Fujimoto, J.K. Ranka, R.S. Windeler, *Opt. Lett.* **26**, 608 (2001)
- 9 C. Dunsby, P.M.P. Lanigan, J. McGinty, D.S. Elson, J. Requejo-Isidro, I. Munro, N. Galletly, F. McCann, B. Treanor, B. Onfelt, D.M. Davis, M.A.A. Neil, P.M.W. French, *J. Phys. D* **37**, 3296 (2004)
- 10 G. McConnell, *Opt. Express* **12**, 2844 (2004)
- 11 J. Chou, Y. Han, B. Jalali, *Photon. Technol. Lett.* **16**, 1140 (2004)
- 12 J.W. Walewski, S.T. Sanders, *Appl. Phys. B* **79**, 415 (2004)
- 13 S. Moon, D.Y. Kim, *Opt. Express* **14**, 11 575 (2006)
- 14 J.M. Dudley, G. Genty, S. Coen, *Rev. Mod. Phys.* **78**, 1135 (2006)
- 15 J.K. Ranka, R.S. Windeler, A.J. Stentz, *Opt. Lett.* **25**, 25 (2000)
- 16 I. Thomann, A. Bartels, K.L. Corwin, N.R. Newbury, L. Hollberg, S.A. Diddams, J.W. Nicholson, M.F. Yan, *Opt. Lett.* **28**, 1368 (2003)
- 17 C. Lin, R.H. Stolen, *Appl. Phys. Lett.* **28**, 216 (1976)
- 18 A.N. Gur'yanov, D.D. Gusovskii, E.M. Dianov, E.A. Zakhidov, A.Y. Katsik, *Kvant. Elektron. (Moskva)* **12**, 799 (1985)
- 19 S.N. Chernikov, Y. Zhu, J.R. Taylor, *Opt. Lett.* **22**, 5 (1997)
- 20 J.W. Walewski, J.A. Filipa, C.L. Hagen, S.T. Sanders, *Appl. Phys. B* **83**, 75 (2006)
- 21 L.G. Cohen, C. Lin, *IEEE J. Quantum Electron.* **QE-14**, 11 (1978)
- 22 C. Lin, V.T. Ngugen, W.G. French, *Electron. Lett.* **4**, 25 (1978)
- 23 R.J. Bartula, J.W. Walewski, S.T. Sanders, *Appl. Phys. B* **84**, 395 (2006)
- 24 C. Xia, M. Kumar, O.P. Kulkarni, M.N. Islam, F.L. Terry Jr., *Opt. Lett.* **13**, 17 (2006)
- 25 C.L. Hagen, J.W. Walewski, S.T. Sanders, *Photon. Technol. Lett.* **18**, 91 (2006)
- 26 M.G. Allen, E.R. Furlong, R.K. Hanson, Tunable diode laser sensing and combustion control, in *Applied Combustion Diagnostics*, ed. by K. Kohse-Hoinghaus, J.B. Jeffries (Taylor & Francis, New York, 2002)
- 27 G.P. Agrawal, *Nonlinear Fiber Optics*, 4th edn. (Academic, San Diego, CA, 2007)
- 28 L.S. Rothman, D. Jacquemart, A. Barbe, D.C. Benner, M. Birk, L.R. Brown, M.R. Carleer, C. Chackerian Jr., K. Chance, V. Dana, V.M. Devi, J.-M. Flaud, R.R. Gamache, A. Goldman, J.-M. Hartmann, K.W. Jucks, A.G. Maki, J.-Y. Mandin, S.T. Massie, J. Orphal, A. Perrin, C.P. Rinsland, M.A.H. Smith, J. Tennyson, R.N. Tolchenov, R.A. Toth,

- J. Vander Auwera, P. Varanasi, G. Wagner, J. Quant. Spectrosc. Radiat. Transf. **96**, 139 (2005)
- 29 M. Bach, R. Georges, M. Herman, A. Perrin, Mol. Phys. **97**, 265 (1999)
- 30 A. Boschetti, D. Bassi, E. Iacob, S. Iannotta, L. Ricci, M. Scotoni, Appl. Phys. B **74**, 273 (2002)
- 31 S.T. Sanders, L. Ma, J. Jefferies, R.K. Hanson, Proc. Combust. Inst. **49**, 161 (2002)
- 32 J. Hult, R.S. Watt, C.F. Kaminski, Opt. Express **15**, 11 385 (2007)
- 33 C.L. Hagen, *Fundamentals of Transient Thermal-Light Absorption Spectroscopy and Application of Optical Sensing in HCCI Engines, Chapter 2 – Optical Noise*, Ph.D. (Mechanical Engineering) thesis, University of Wisconsin-Madison (2006)
- 34 X. Liu, J.B. Jeffries, R.K. Hanson, Am. Inst. Aeronaut. Astronaut. J. **45**, 411 (2007)